Available online at www.sciencedirect.com
SCIENCE DIRECT
Journal of Molecular Catalysis A: Chemical 248 (2006) 113–120
JOURNAL OF MOLECULAR CATALYSIS A: CHEMICAL
www.elsevier.com/locate/molcata

Beta zeolite supported on a β-SiC foam monolith: A diffusionless catalyst for fixed-bed Friedel–Crafts reactions

Gauthier Winé [a], Jean-Philippe Tessonnier [a], Séverinne Rigolet [b], Claire Marichal [b], Marc-Jacques Ledoux [a], Cuong Pham-Huu [a,*]

[a] *Laboratoire des Matériaux (Part of the ELCASS (European Laboratory of Catalysis and Surface Science)), Surfaces et Procédés pour la Catalyse (LMSPC), UMR 7515 du CNRS, ECPM-ULP, 25 rue Becquerel, F-67087 Strasbourg Cedex 2, France*

[b] *Laboratoire de Matériaux à Porosité Controlée (LMPC), UMR 7016 du CNRS, ENSCMu-UHA, 3 rue Alfret Werner, F-68093 Mulhouse Cedex, France*

Received 5 October 2005; received in revised form 7 December 2005; accepted 12 December 2005
Available online 20 January 2006

Abstract

Binderless beta zeolite has been anchored on a silicon carbide foam with a monolithic shape. The catalytic activity of the resulting composite was evaluated for a Friedel–Crafts reaction carried out in a fixed-bed configuration: the benzoylation of anisole to *p*-methoxybenzophenone. The results obtained were compared with those of a commercial beta zeolite. Significantly higher product yields along with a stable activity were obtained with the BEA/SiC composite. It has been suggested that the opened structure of the β-SiC foam and the absence of any binder allow a fast desorption of the *p*-ketone which is the main product of the reaction but also the major source of deactivation due to strong adsorption and/or coke formation inside the microporosity of the zeolite.

Keywords: Acylation; Friedel–Crafts reaction; Fixed-bed; Beta zeolite; Beta silicon carbide; Monolith

1. Introduction

Zeolite materials are widely employed in industrial processes such as catalysis, adsorption and separation [1,2]. Their synthesis is usually carried out under hydrothermal conditions and leads typically to a powder [3]. The small size of the zeolitic particles generates several problems. First, it renders the recovery of the zeolite and its purification difficult. Often ultracentrifugation is needed for the final separation. Secondly, the obtained powder is difficult to handle and to use, especially as catalyst, because of the important pressure drop it causes inside the reactor. Therefore, zeolite powders are often mixed with binders such as α-Al_2O_3 or alumina–silica materials and receive a macroscopic shaping into extrudates or tablets. Unfortunately, the presence of binders significantly hinders (i) the diffusion of the reactants toward the zeolite active sites and (ii) the evacuation of the formed products from the microporous structure. The presence of binders also modifies the zeolite pore volume and its acidic properties [4]. For all these reasons, supporting zeolites onto a carrier with controlled macroscopic shape has received a growing scientific and economic interest during the last decade [5–11]. The use of a macroscopic support is interesting at two different levels. First, the catalyst synthesis becomes easier: the steps of filtration/ultracentrifugation, as well as the mixing with binders and extrusion are no longer needed. Secondly, it lowers the pressure drop and improves the mass transfer and accessibility compared to the bulk form, especially for fast liquid or gas/liquid phase reactions as well as for trickle-bed reactions.

The Friedel–Crafts acylation reaction of aromatic compounds represents one of the most important methods of production of aromatic ketones, which are intermediate products in several fine chemical processes which include the pharmaceutical, agrochemical and fragance industries. Several reports have recently been published on the replacement of traditional $AlCl_3$ or $FeCl_3$ homogeneous catalysts by heterogeneous solid acids, like zeolites, in order to improve the catalyst/products separation and also to reduce the formation of waste and corrosion [10,12–14]. However, most reports deal with the slurry reactor configuration and only very few are devoted to the use of the continuous fixed-bed configuration [15,16] despite the existence of a com-

* Corresponding author.
E-mail address: cuong.lcmc@ecpm.u-strasbg.fr (C. Pham-Huu).

1381-1169/$ – see front matter © 2006 Elsevier B.V. All rights reserved.
doi:10.1016/j.molcata.2005.12.010

mercial re-circulating fixed-bed reactor process operated by Rhodia [17,18]. The real advantage of the fixed-bed compared to the batch configuration is that it allows to decrease the product concentration in the reaction medium. The products can consequently easily desorb from the zeolite and avoid secondary reactions, which would lead to lower selectivity, coke formation and finally poisoning and deactivation of the catalyst [19].

Silicon carbide crystallized in the cubic structure (β-SiC) exhibits a high thermal conductivity, a high resistance towards oxidation, a high mechanical strength, a low specific weight and chemical inertness, all properties required to be a good heterogeneous catalyst support [20–22]. It is expected that silicon carbide will be a promising candidate for use as support for zeolites in place of classical supports such as alumina or silica, especially for highly endothermic and/or exothermic reactions where the precise control of the temperature inside the catalyst bed is extremely important. The chemical inertness of the SiC support allows to avoid any secondary reaction between the support and the synthesis medium. Finally, the extreme lightness of the SiC allows to limit in a significant manner the overall weight increase due to the support when compared to other traditional ceramic materials. The β-SiC with medium surface area can be also synthesized in a foam monolith structure, which offers several advantages when used in catalytic reactions. The open structure of the foam monolith provides a low-pressure drop and high diffusivity of both the reactants and products through the catalytic bed. Monolith catalysts have been widely employed in several catalytic reactions where a high velocity of the reactants per reactor volume unit is required. Recently, reports on the use of monolithic supports to anchore zeolitic materials have been published, which highlight the benefits of the combination of the high accessible surface of the monolith with the dispersed zeolite without any need for washcoat or binders [10].

The aim of the present work is to report the use of the silicon carbide foam monolith supported H-BEA zeolite as catalyst for Friedel–Crafts reactions carried out in the fixed-bed configuration. Activity and stability of this new catalyst are compared with the results obtained with a bulk commercial H-BEA zeolite.

2. Experimental section

2.1. β-SiC material

Silicon carbide (β-SiC) in a monolithic foam form (diameter 20 mm, length 60 mm) with a specific surface area of 7 $m^2\ g^{-1}$ and a mesopore distribution centered at around 40 nm was used as support for the zeolite. The macropores were centered at around 600 μm. The support was synthesized according to a gas–solid reaction between SiO and carbon, which were intimately mixed together inside the material precursor [20]. Briefly, a polyurethane foam was impregnated with an intimate mixture of phenolic resine and silicon powder. The resine was then polymerised and carbonised at 200 °C several hours. Finally, the silicon containing carbon skeleton obtained was carburised at 1400 °C in order to form the β-SiC foam. Part of the SiC was covered with a thin amorphous layer (Fig. 1(A)), which was constituted by a mixture of SiO_2 and SiO_xC_y while the other part was a clean SiC surface (Fig. 1(B)) according to the XPS analysis (Fig. 1(C)). Before zeolite deposition, the foam monolith of SiC was calcinated in air at 900 °C for 2 h in order to transform the SiO_xC_y phase into a homogeneous SiO_2 layer [21,22].

2.2. H-BEA/SiC foam composite synthesis

The supported zeolite synthesis was carried out in an hydrothermal mode using the following precursor solution composition—SiO_2:Al_2O_3:TEAOH:H_2O (50:1:14:370) according to the method already described previously [23]. The gel was transferred into a Teflon-lined autoclave (100 ml capacity). The foam of β-SiC was immersed inside the zeolite gel precursor and the autoclave was heated at 140 °C for 48 h. After synthesis, the foam was removed and sonicated several times with water in order to remove the weakly adsorbed zeolite from its surface. The organic template (tetraethylammonium hydroxyde, TEAOH) was removed by heating the sample in flowing argon at 550 °C for 14 h. The as-prepared beta zeolite/SiC was then ion-exchanged overnight with NH_4Cl (1 M, 150 ml) at 90 °C to obtain the NH_4-form. The H-beta form was finally obtained by calcination of the sample in air at 550 °C for 10 h. The resulting H-BEA had a Si:Al ratio of 25.

For comparison, a commercial H-BEA zeolite (Zeolyst International, batch CP814E, Si:Al ratio of 12.5 according to the information given by the producer) was also tested under the same reaction conditions. The H-BEA was obtained by calcinating the commercial NH_4-BEA in air at 550 °C for 10 h. The powder was then pasted and crushed in order to obtain grains between 0.4 and 1 mm in diameter.

2.3. Fixed-bed Friedel–Crafts reaction

The catalytic test was carried out in the fixed-bed configuration. The same amount of catalyst was blocked between quartz wool plugs in a vertical quartz reactor (inner diameter 20 mm, length 300 mm) located in a vertical electrical furnace. The reactant mixture, anisole and benzoyl chloride with a molar ratio of 8 (Fig. 2), was injected into the reactor through a HPLC pump (Varian Model 9002) with a liquid rate of 0.1 ml min^{-1} corresponding to a weight hourly space velocity (WHSV) of 4 h^{-1}. The amout of catalyst used were 0.4 g for the commercial BEA, and 4 g for the composite BEA/SiC.

2.4. Characterisation techniques

SEM observation was carried out on a field emission scanning microscope model Jeol JSM-6700F working under low accelerated voltage, 3–15 kV, and allowing the microstructural investigation down to a few nanometers size.

BET surface areas were measured by means of a commercial BET unit (Coulter SA 3100, Coultronic SA) using N_2 adsorption at 77 K. Before the N_2 adsorption, samples were heated at 325 °C for 14 h under dynamic vacuum in order to desorb the impurities or moisture adsorbed on the surface or inside the microporosity of the zeolite.

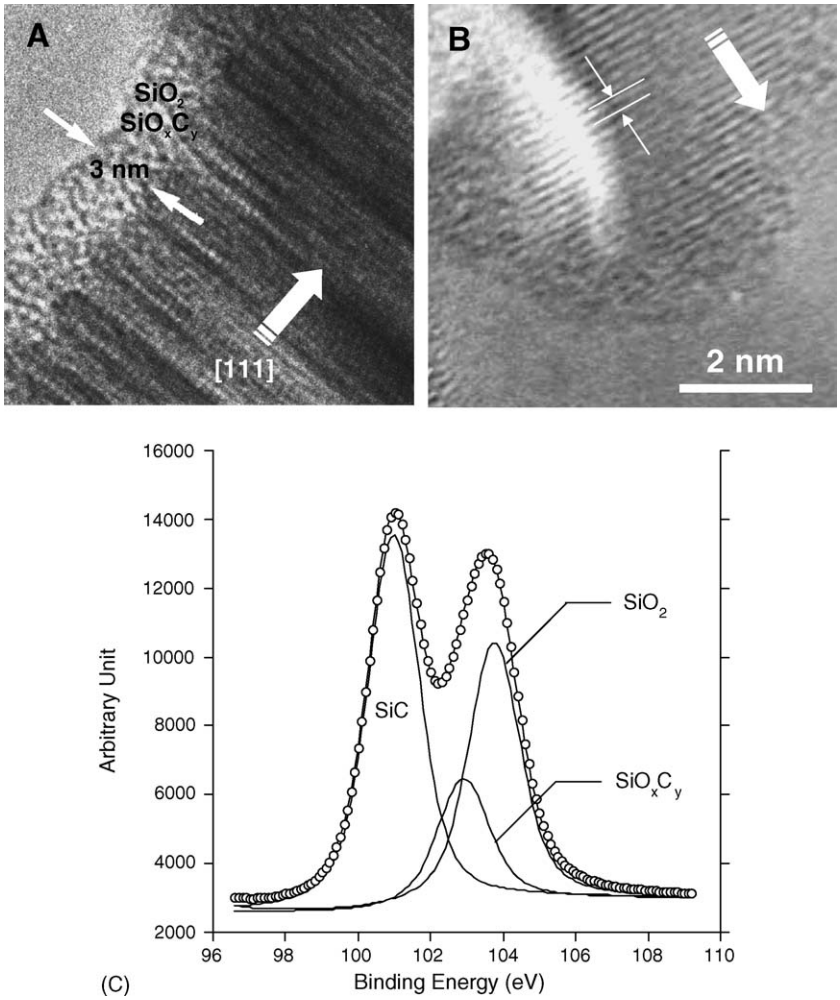

Fig. 1. High-resolution TEM images showing the duality of the SiC surface: (A) SiC surface covered with a thin amorphous layer constituted by a mixture of SiO_2 and SiO_xC_y, (B) clean SiC surface, and (C) corresponding XPS spectrum showing the presence of the different Si-based phases.

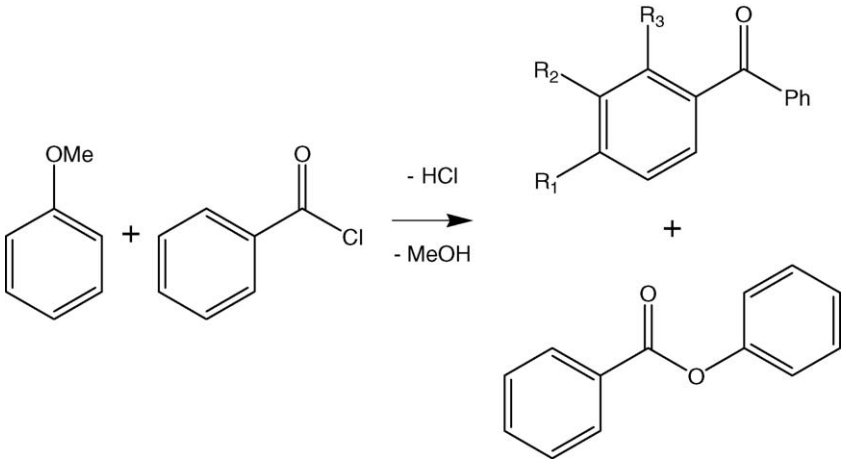

Fig. 2. Reaction path of the Friedel–Crafts reaction of anisole benzoylation to *p*-methoxybenzophenone. The reaction of anisole and benzoyl chloride produces cetones, *o*-methoxybenzophenone (R_1 = H, R_2 = H, R_3 = OMe), *m*-methoxybenzophenone (R_1 = H, R_2 = OMe, R_3 = H), *p*-methoxybenzophenone (R_1 = OMe, R_2 = H, R_3 = H), and one ester, the phenyl benzoate. The secondary products are HCl and methanol, respectively, when cetone and ester are formed.

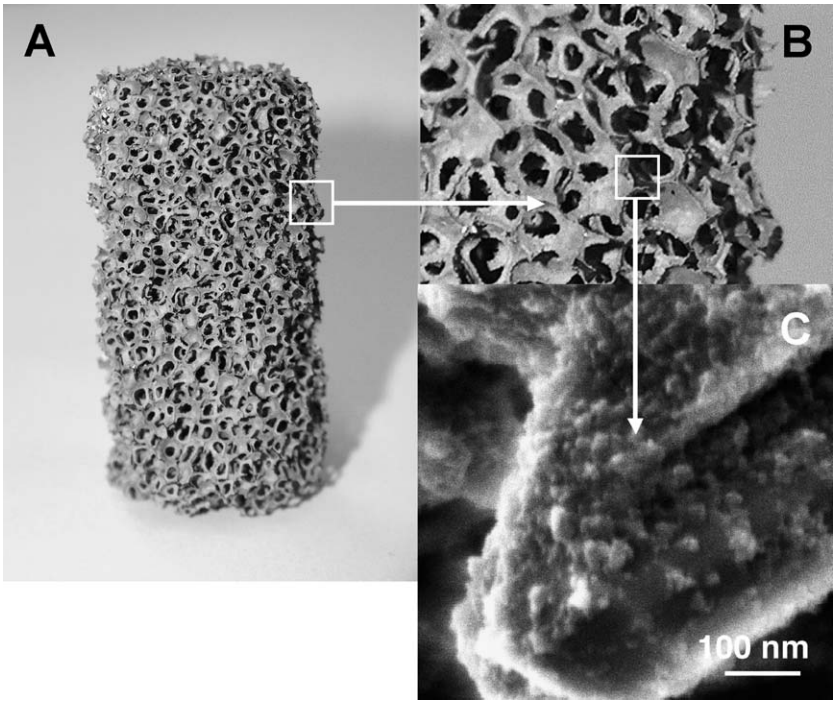

Fig. 3. Optical and SEM images of the H-BEA/SiC composite. The homogeneous and small size of the deposited zeolite can be seen in (C).

^{27}Al ($I = 5/2$) magic angle spinning nuclear magnetic resonance (MAS-NMR) was carried out with a Brucker DSX 400 spectrometer operating at $B_0 = 9.4$ T (Larmor frequency $\nu_0 = 104.2$ Mhz). A single pulse of 0.8 μs with a recycle delay of 1 s was used for all experiments. The spinning frequency was 8 kHz. Measurements were carried out at room temperature with $[Al(H_2O)_6]^{3+}$ as external standard reference. Before measurements the sample was re-hydrated at room temperature for overnight.

The crystallinity of the different samples was investigated with the powder X-ray diffraction technique (XRD) carried out on a Siemens D-5000 diffractometer using a non-monochromatic Co Kα radiation ($\lambda = 0.1789$ nm). The average particle size was calculated from the X-ray line broadening using the Scherrer equation assuming that the particles are spherical.

The temperature-programmed oxidation (TPO) were carried out on a 200 mg sample, under a flow of O_2 (10% in He) at 50 cm^3/min, from room temperature to 800 °C at 10 °C/min. A Saturn 3 Varian mass spectrometer was used to analyse the outlet gas-phase composition and to follow the signal of CO ($m/e = 28$) and CO_2 ($m/e = 44$). Calibration was realised using known amounts of Mo_2C. For each sample, the results were normalized versus the amount of zeolite.

3. Results and discussion

3.1. H-BEA/SiC composite characteristics

Optical images of the starting SiC support foam (Fig. 3(A) and (B)) clearly show the high macroscopic void fraction throughout the monolith matrix. The specific surface area measured by N_2 adsorption at liquid nitrogen temperature is 7 m^2 g^{-1} and was mainly composed by meso- and macro-pores according to the N_2 adsorption isotherm (mesopores measurements) and to the mercury titration (macropores measurements). The zeolite deposit, determined by HF treatment, was about 10 wt.% which is in good agreement with the previous results obtained under similar synthesis conditions on the SiC grain size or extrudate [24].

The purity of the SiC-supported zeolite was checked by means of the ^{27}Al MAS-NMR technique (Fig. 4) which showed that all the aluminium was engaged in the zeolite framework, i.e. tetrahedral coordination, and only a small trace of extraframework aluminium or distorded aluminium has been observed [25]. The NMR spectrum corresponding to the commercial H-BEA zeolite was also reported in the same figure for comparison. The full width at half maximum (FWHM) of the ^{27}Al band was around 10 ppm. According to van Grieken et al. [26] and Jacobsen et al. [25] this value reflects a relatively low crystal size of the as-prepared zeolite, which confirms the XRD results of the present work. Jacobsen et al. [25] have reported a FWHM of 7.1 ppm for large ZSM-5 crystals (8 μm), whereas for small size ZSM-5 crystals (nanometer size) the FWHM significantly increased to about 10.6–11.1 ppm. The average zeolite particle size determined by the NMR results is also in good agreement with that observed by SEM (Fig. 3(C)).

In a previous work [24,27] we showed that the zeolite anchorage was extremely strong as almost no zeolite loss has been observed after submitting the sample to a sonication treatment for 30 min. The high mechanical anchorage was attributed to a chemical binding between the first layer of the zeolite with the oxygenated compounds, i.e. SiO_2 and SiO_xC_y, on the SiC support surface. During the contact with the zeolite precursor gel it was expected that part of the SiO_2–SiO_xC_y phase was dis-

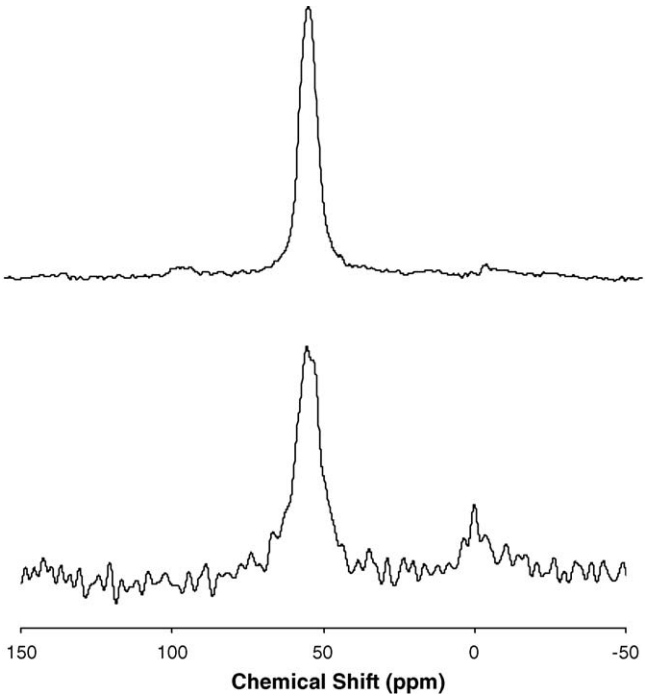

Fig. 4. ^{27}Al MAS-NMR spectra of the H-BEA/SiC foam composite after synthesis and template removal and a commercial H-BEA zeolite.

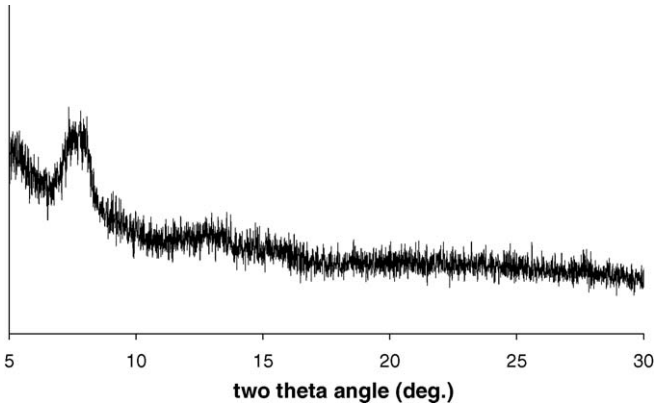

Fig. 6. XRD pattern of the H-BEA/SiC composite of the present work.

solved leading to the formation of an interface with high Si/Al ratio. Such interface has been reported recently by Ulla et al. [9] to have an extremely high wettability towards solid surface even with low reactivity, i.e. cordierite, which in turn, provides an anchorage phase for the subsequent growth of zeolite with a lower Si/Al ratio. In the case of SiC with a layer of SiO_2 on the surface, the formation of the Si-rich gel layer and the subsequent growth of the zeolite with lower Si/Al ratio was expected to occur almost instantaneously leading to the formation of a relatively high amount of zeolite with high anchorage stability on the SiC surface. A schematic illustration of such proposed growth sequence is displayed in Fig. 5.

Optical image (Fig. 3(A)) shows that the macroscopic shape of the support was not modified during the synthesis even in a highly basic medium. Medium magnification (Fig. 3(B)) shows that zeolite was well dispersed on the SiC surface as no trace of any aggregates of zeolite has been observed. High-resolution SEM image (Fig. 3(C)) clearly shows the presence of small zeolite particles homogeneously dispersed on a large part of the surface of the support. The zeolite particles were in a round-shaped form with a mean diameter centered at around 30 nm, which is in good agreement with the nanosized beta zeolite reported in the literature [28].

The deposition of zeolite on the SiC surface significantly increases the overall specific surface area of the material, i.e. 47 $m^2\,g^{-1}$ instead of 7 $m^2\,g^{-1}$ for the starting monolith support, along with a large microporous contribution according to the N_2 adsorption isotherm. Taking into account the unmodified surface area of the starting SiC support the real specific surface area of the deposited zeolite was about 400 $m^2\,g^{-1}$ which was in good agreement with the surfaces generally obtained with zeolitic materials in the literature [28].

The XRD pattern of the as-synthesized sample is presented in Fig. 6. It only shows the presence of a large peak at around 8°, which is usually characteristic of an amorphous phase. Such diffraction line has already been reported by Jacobs et al. [29] during their study on the ZSM-5 zeolite and was attributed to the presence of very small zeolite particles encapsulated inside an amorphous silica or alumina framework. Same observation was also reported by Camblor et al. [28] during their study on the synthesis of small BEA zeolite crystals (8 nm). Ulla et al. [9] have reported that the zeolite nucleation rate was faster in the bulk of the synthesis gel than in the gel layer coating the solid support. Such phenomenon could favorize the formation

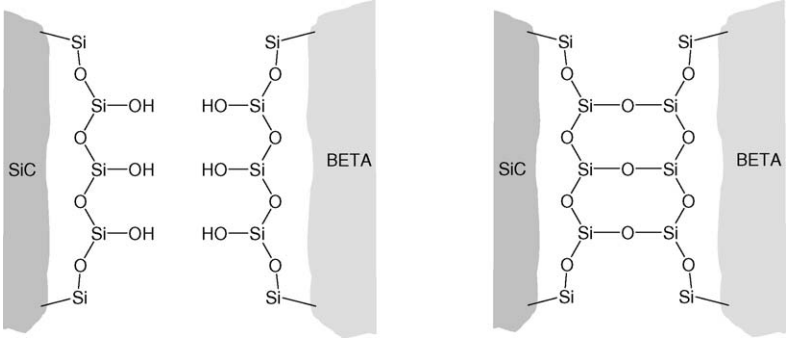

Fig. 5. Scheme of the SiC–zeolite interface and the mode of zeolite anchorage owing to the presence of an oxygen-content silicon layer. It was expected that this mode of anchorage allows to increase the mechanical resistance of the deposited zeolite on the SiC support surface.

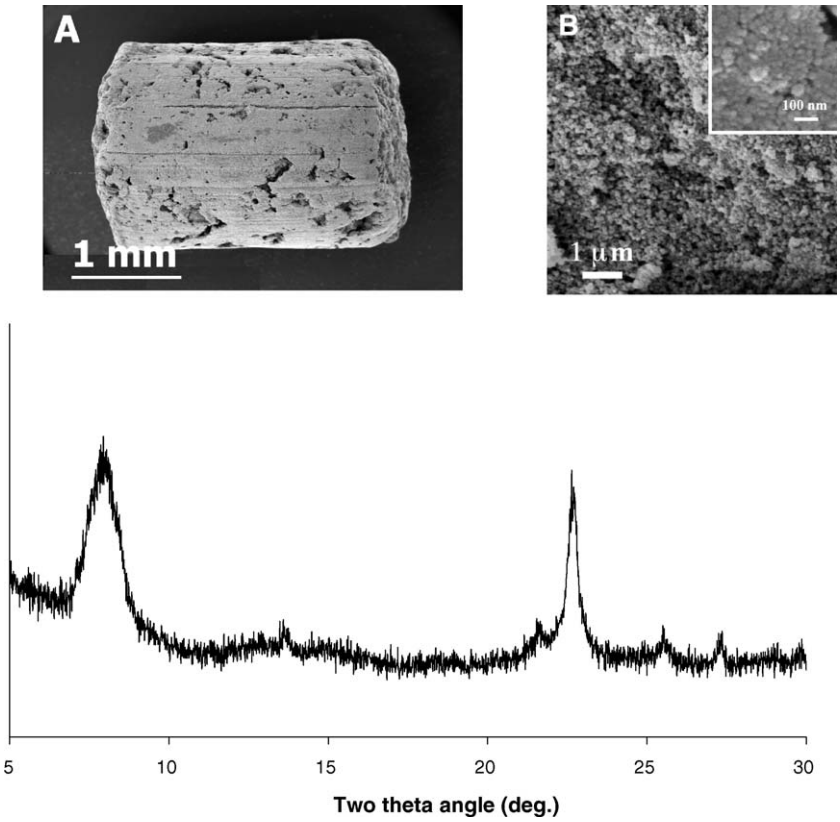

Fig. 7. SEM images and XRD pattern of H-BEA/SiC extrudates.

of crystallized zeolite particles with bigger size in the solution while smaller zeolite crystals would coat the solid support thus giving a broad X-ray diffraction line.

It is worth noting that BEA synthesis carried out using β-SiC in an extrudate form under similar reaction conditions gives rise to the formation of well crystallized zeolite particles (Fig. 7). The difference in the zeolite crystallinity observed on the two β-SiC supports could be due to a difference in the surface reactivity or the specific surface area.

3.2. Catalytic activity

A blank test, first carried out on the SiC support alone, showed no catalytic activity which is in line with the chemical inertness of the support. The catalytic activity and selectivity obtained for the Friedel–Crafts reaction carried out in a fixed-bed configuration at 120 °C as a function of time on stream are presented in Fig. 8. The benzoylation activity obtained on the BEA/β-SiC foam catalyst was high at the beginning, 95%, and then slowly decreased with time on stream to stabilize at about 60% after 10 h on stream. The benzoylation activity and selectivity obtained under the same reaction conditions on the commercial bulk beta zeolite are also reported for comparison (Fig. 8). The initial benzoylation activity of the commercial zeolite was similar to that observed with the supported catalyst, i.e. 75% after 1 h on stream. However, the activity drastically decreased from 70% to less than 20% after 8 h on stream indicating a strong inhibition of the active site leading to a drastic deactivation.

The selectivity towards *p*-methoxybenzophenone remains high, i.e. 95%, and unchanged as a function of time on stream which indicates that the nature of the catalysts was not modified during the course of the test. The other reaction products, i.e. *o*-methoxybenzophenone and ester were formed in almost equal concentrations and represented less than 4% of the total reac-

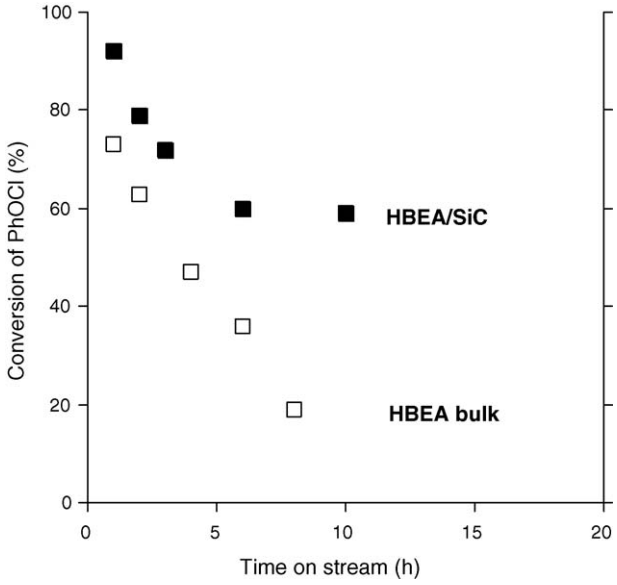

Fig. 8. Catalytic results for the Friedel–Crafts benzoylation over H-BEA/SiC and commercial H-BEA catalysts at 120 °C in a fixed-bed mode with a WHSV of 4 h^{-1}.

tion products. The observed results are in good agreement with those reported by different authors in the literature [30]. Previous catalytic tests performed in our group with BEA zeolites synthesized in the same conditions but presenting Si/Al ratios between 12.5 and 100 have shown that, for the benzoylation of anisole, the acidity of the zeolite has neither influence on the conversion nor on the deactivation rate [31]. Therefore, the high benzoylation activity observed on the SiC supported beta zeolite compared to that of the bulk beta zeolite was attributed to the dispersion of the zeolite particles on the surface of the support which allows the fast diffusion of the reactants towards the catalyst and the rapid evacuation of the aromatic ketone product from the microporosity to the liquid medium.

3.3. About the deactivation mode

The rapid deactivation slope observed on the commercial bulk H-BEA was attributed to the site blockage due to the accumulation of heavier products. It has been reported by several authors that the aromatic ketone, i.e. *p*-methoxybenzophenone, is the main inhibitor for the Friedel–Crafts reaction due to its strong adsorption on the active sites. Derouane et al. [19] have reported that the acylation activity over bulk H-BEA zeolite significantly decreased as the amount of aromatic ketone in the reactant mixture increased. A similar deactivation has also been reported by Jaimol et al. [15] in a fixed-bed reactor during the acetylation of toluene over H-ZSM5 catalyst. At 453 K the conversion decreased from 70% to 30% after about 7 h on stream. The deactivation observed was attributed by the authors to coke formation inside the zeolite microporosity. The accumulation of the heavier products inside the zeolite microporosity was also enhanced by the absence of solvent in the reactants mixture, which significantly lowers the extraction rate resulting to an accelerated deactivation. Apparently, because of the accumulation of the aromatic ketone inside the zeolite porosity, the real stoichiometry of the different reactants inside the zeolite cavity was modified which in turn, lowered the catalytic activity with time on stream. It is also noted that the difficulty in evacuating the heavier products formed inside the zeolite cavity also probably increased the coke formation through acidic condensation, thus leading to deactivation by site encapsulation. The relatively short contact time in the fixed-bed configuration also contributes to the apparent deactivation as the products have less time to be extracted in comparison to the slurry configuration. It has been reported by Derouane [32] that the partition between the reactants and products between the zeolite porosity and the bulk solvent plays an important role in the stability of the catalytic activity. Low products extraction could also lead to deactivation due to the dealumination of the zeolite by products, i.e. HCl in the present work.

Temperature-programmed oxidation (TPO) analyses carried out on the commercial catalyst clearly highlights the important coke formation when compared to that which was observed on the SiC supported H-BEA catalyst, i.e. 7 wt.% instead of 1.25 wt.% (Fig. 9). In addition, the coke formed on the bulk zeolite catalyst also exhibits a higher resistance towards combustion, i.e. maximum combustion peak at 600 °C instead of 400 °C for the supported zeolite. Apparently, low diffusional escaping of the heavy products inside the pores of the bulk zeolite induces the formation of coke with a higher graphitic character.

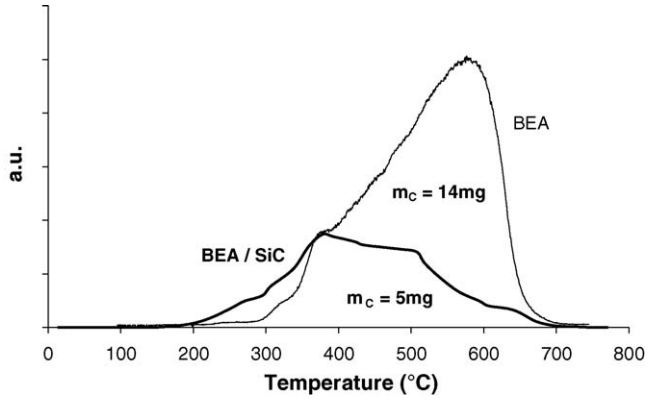

Fig. 9. TPO spectra (CO_2 with a $m/z = 44$) obtained on the H-BEA/SiC and commercial H-BEA after Friedel–Crafts reaction.

In fact, the dispersion of the zeolite cristals on the SiC support also allows a high diffusion rate of ketones out of the (zeolite) porosity of the BEA/SiC catalyst, thus conducing to a lower deactivation rate as a function of time on stream when compared to that observed on the bulk beta zeolite. Optimisation work is on-going to diminish the deactivation as a function of time on stream by modifying the cell porosity of the β-SiC foam and will be presented soon.

4. Conclusion

In summary, we have shown that β-SiC is a promising material for supporting zeolites. Besides its intrinsic advantages, i.e. high strength and high thermal conductivity, β-SiC allows a chemical binding of the zeolite on its surface thus minimising the zeolite loss during the reaction. Furthermore, the macroscopic shape of the β-SiC can be tuned, from powder to monolithic foam, depending on the subsequent application.

In the present work, BEA zeolite has been anchored on a β-SiC foam monolith and the catalytic activity of the resulting composite has been evaluated for a Friedel–Crafts reaction. The supported H-BEA/SiC catalyst was extremely active, selective and stable for the benzoylation of anisole by benzoyl chloride in a fixed-bed configuration when compared to the results obtained on the commercial bulk beta zeolite. The stability of the supported zeolite was attributed to the high external surface, which allows the rapid evacuation of the heavy ketone products. The use of SiC in a monolithic shape allows to reduce in a large extend the problems of diffusion which is not easy with a traditional support shape, especially in a trickle-bed mode. On the bulk zeolite the difficulty encountered with the heavy ketone products evacuation led to the progressive encapsulation of the active sites, thus resulting to a rapid deactivation.

References

[1] H.L. Hoffman, L. Riddle, Hydrocarbon Process. Int. Ed. 67 (1988) 41.

[2] M. Guisnet, J.-P. Gilson, Zeolites for Cleaner Technologies, Imperial College Press, London, 2002.
[3] R.M. Barrer, Hydrothermal Chemistry of Zeolites, Academic Press, London, 1987.
[4] X. Wu, A. Alkhawaldeh, R.G. Antony, Stud. Surf. Sci. Catal. 143 (2002) 217.
[5] N. van der Puil, F.M. Dautzenberg, H. van Bekkum, J.C. Jansen, Micropor. Mesopor. Mater. 27 (1999) 95.
[6] Z. Shan, W.E.J. van Kooten, O.L. Oudshorn, J.C. Jansen, H. van Bekkum, C.M. van den Bleek, H.P.A. Calis, Micropor. Mesopor. Mater. 34 (2000) 81.
[7] G.B.F. Seijger, O.L. Oudshorn, W.E.J. van Kooten, J.C. Jansen, H. van Bekkum, C.M. van den Bleek, H.P.A. Calis, Micropor. Mesopor. Mater. 39 (2000) 195.
[8] G.B.F. Seijger, A. van den Berg, R. Riva, K. Krishna, H.P.A. Calis, H. van Bekkum, C.M. van den Bleek, Appl. Catal. A 236 (2002) 187.
[9] M.A. Ulla, R. Mallada, J. Coronas, L. Gutierrez, E. Miro, J. Santamaria, Appl. Catal. A 253 (2003) 257.
[10] A.E.W. Beers, T.A. Nijhuis, N. Aalders, F. Kapteijn, J.A. Moulijn, Appl. Catal. A 243 (2003) 237.
[11] O. Öhrman, J. Hedlund, J. Sterte, Appl. Catal. A 270 (2004) 193.
[12] Y. Ma, Q.L. Wang, W. Jiang, B. Zuo, Appl. Catal. A 165 (1997) 199.
[13] C. Guignard, V. Pédron, F. Richard, R. Jacquot, M. Spagnol, J.M. Coustard, G. Pérot, Appl. Catal. A 234 (2002) 79.
[14] V.R. Choudhary, S.K. Jana, J. Mol. Catal. A 180 (2002) 267.
[15] T. Jaimol, A.K. Pandey, A.P. Singh, J. Mol. Catal. A 170 (2001) 117.
[16] K.G. Bhattacharyya, A.K. Talukdar, P. Das, S. Sivasanker, Catal. Commun. 2 (2001) 105.
[17] M. Spagnol, L. Gilbert, E. Benazzi, C. Marcilly, US Patent 6,013,840, assigned to Rhodia Chimie, 2000.
[18] M. Spagnol, L. Gilbert, H. Guillot, P.J. Tirel, US Patent 6,194,616, assigned to Rhodia Chimie, 2001.
[19] E.G. Derouane, G. Crehan, C.J. Dillon, D. Bethell, H. He, S.B. Derouane-Abd Hamid, J. Catal. 194 (2000) 410.
[20] M.J. Ledoux, S. Hantzer, C. Pham-Huu, M.P. Desaneaux, J. Guille, J. Catal. 114 (1988) 176.
[21] C. Pham-Huu, M.J. Ledoux, CaTTech 5 (2001) 226.
[22] C. Pham-Huu, N. Keller, M.J. Ledoux, L'actualité Chimique 8 (2002).
[23] G. Winé, J.P. Tessonnier, C. Pham-Huu, M.J. Ledoux, Chem. Commun. 20 (2002) 2418.
[24] S. Basso, J.P. Tessonnier, G. Winé, C. Pham-Huu, M.J. Ledoux, US Patent Application 20030162649, assigned to Sicat, 2003.
[25] C.J.H. Jacobsen, C. Madsen, T.V.W. Janssens, H.J. Jakobsen, J. Skibsted, Micropor. Mesopor. Mater. 39 (2000) 393.
[26] R. van Grieken, J.L. Sotelo, J.M. Menéndez, J.A. Melero, Micropor. Mesopor. Mater. 39 (2000) 135.
[27] G. Winé, J.P. Tessonnier, A.C. Faust, S. Rigolet, C. Marichal, C Pham-Huu, M.J. Ledoux, Appl. Catal. A, submitted for publication.
[28] M.A. Camblor, A. Corma, S. Valencia, Micropor. Mesopor. Mater. 25 (1998) 59.
[29] P.A. Jacobs, E.G. Derouane, J. Weitkamp, J. Chem. Soc., Chem. Commun. 12 (1981) 591.
[30] M. Chidambaram, C. Venhatesan, P. Moreau, A. Finiels, A.V. Ramaswany, A.P. Singh, Appl. Catal. A 224 (2002) 129.
[31] G. Winé, PhD Thesis, Université L. Pasteur, Strasbourg (France), 2004.
[32] E.G. Derouane, CaTTech 5 (2001) 214.